

Generation of Entangled Ancilla States for use in Linear Optics Quantum Computing

J.D. Franson, M. M. Donegan, and B.C. Jacobs
Johns Hopkins University
Applied Physics Laboratory
Laurel, MD 20723

Abstract:

We describe several different methods for generating the entangled ancilla states that are required for linear optics quantum computing. We show that post-selection can be used in combination with linear optical elements to generate the entangled ancilla, but with an exponentially-small efficiency. Alternatively, the ancilla can be efficiently generated using solid-state devices consisting of quantum wells coupled with tunnel junctions. Finally, we consider the possibility of using encoded ancilla in order to reduce the effects of decoherence and measurement errors.

I. INTRODUCTION

Quantum logic operations can be performed using linear optical elements, such as beam splitters and phase shifters, combined with measurements made on a set of n entangled ancilla photons. In the original approach suggested by Knill, Laflamme, and Milburn (KLM) [1], post-selection can be used to obtain the correct logical output with a failure rate that scales as $2/(n+1)$. We have subsequently shown [2] that the entangled ancilla state can be chosen in such a way as to maximize the fidelity of the output with an error rate that scales as $4/(n+1)^2$. In either case, a practical implementation of linear optics quantum computing will require a method for generating the appropriate entangled ancilla states for a sufficiently large value of n and with an error rate below the threshold for fault-tolerant computation.

Here we consider several different methods for generating the required ancilla states. The most obvious approach is to use linear optical elements and post-selection. We present a straightforward method for generating the required ancilla using post-selection in Section III, but we find that the efficiency of this method decreases exponentially with n . We have not proven that this approach is optimal, however, and it is possible that more efficient algorithms may eventually be found.

In Section IV, we outline a method for generating the entangled ancilla photon states using solid-state techniques. A series of quantum wells are coupled using tunnel junctions and the Coulomb blockade effect [3, 4] to produce an entangled electronic state. The algorithm is analogous to the one used for post-selection, except that all of the necessary operations can be performed with high efficiency. Once the electrons have been generated in the desired entangled state, they would be converted into photonic qubits using high-efficiency coupling [5] into a set of single-mode optical fibers.

It would be desirable to be able to use encoded ancilla for quantum logic operations, since that would make the ancilla relatively insensitive to decoherence and other sources of error during their generation, transportation, storage, and measurement. With that in mind, we investigate the possibility of generating and using encoded ancilla in Section V. Although it is possible to introduce logical ancilla that are encoded, we find that the use of unencoded ancilla for the teleportation of the physical qubits appears to be unavoidable. Nevertheless, it may be advantageous to generate the ancilla in encoded form and then decode them for use in the logic gates.

We begin in Section II with a brief review of linear optics quantum computing, including some comments on fault-tolerant computation. Although this paper is not intended as a review article, a brief description of fault-tolerant techniques is required for the discussion of encoded ancilla in Section V. A calculation of the threshold for fault-tolerant computation is beyond the intended scope of this paper, but some general observations will be made regarding the potential advantages and disadvantages of several possible implementations.

II. REVIEW OF LINEAR OPTICS QUANTUM COMPUTING

Gottesman and Chuang [6] showed that quantum logic operations could be performed using quantum teleportation [7] if the desired logic operation was applied to the EPR pairs used in the teleportation before the teleportation was performed. Roughly speaking, the logic operation and the teleportation commute with each other, aside from deterministic single-qubit corrections that may be required. The advantage of this approach is that the modified ancilla state can be prepared in advance using probabilistic techniques that can be repeated until they succeed, after which the teleportation can be done with certainty.

A potential limitation of this approach is the fact that quantum teleportation requires a Bell-state measurement, which cannot be done with certainty using linear optical devices [8, 9]. KLM showed [1] that quantum teleportation could, however, be performed probabilistically using an entangled state of n photons that are distributed between two sets of n optical modes, which we refer to as registers x and y as illustrated in Figure 1. Each register could consist of n single-mode optical fibers, for example.

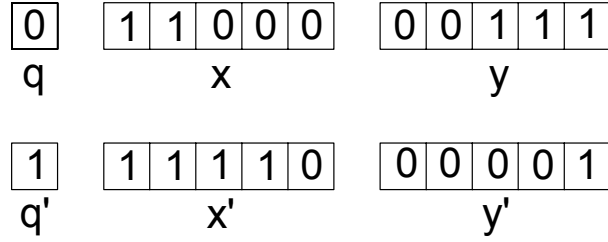


Figure 1. Ancilla registers x and y used in the quantum teleportation of qubit q . Each mode initially contains 0 or 1 photons, while the total number of photons in x and y has a fixed value n ($n = 5$ for the example shown here). The index j in the entangled state of Eq. (1) corresponds to the number of photons in x . Similar ancilla registers x' and y' are used to teleport a second qubit q' during logic operations.

The first step in the teleportation process is to perform a Fourier transform \hat{F} on the combined register c consisting of input qubit q and register x , where \hat{F} is defined by the operator transformation

$$\hat{a}_j^\dagger \rightarrow \frac{1}{\sqrt{n+1}} \sum_{k=0}^n e^{2\pi i j k / (n+1)} \hat{a}_k^\dagger \quad (1)$$

Here the operators \hat{a}_j^\dagger create a photon in the corresponding modes, as usual. It should be noted that \hat{F} is not equivalent to the usual quantum Fourier transform [10], which maps every basis state into every other basis state. The number of photons in each mode of c is measured after the Fourier transform and, based on those results, the teleported output qubit can be selected from one of the modes of register y , as described in detail in

References [1] and [2] and illustrated schematically in Figure 2. The relative phase of the 0 and 1 components of q may require a deterministic correction based on the results of the measurement, which is a form of feed-forward control [11].

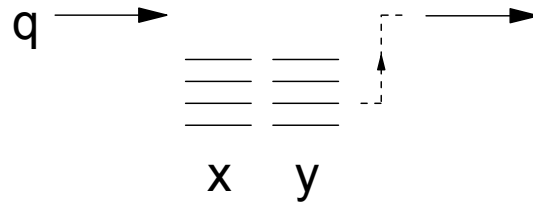


Figure 2. Schematic diagram of the teleportation of qubit q using entangled ancilla registers x and y corresponding to $n = 4$. A Fourier transform is first applied to q and x , after which the number of photons in each of those modes is measured. Based on the results of the measurements, the output qubit is selected from one of the modes of register y as illustrated by the dashed line. A deterministic phase correction may also need to be applied.

Aside from a normalization constant, the entangled state of the ancilla in registers x and y required for the teleportation is given by

$$|\psi_A\rangle = \sum_{j=0}^n f(j) |1\rangle^j |0\rangle^{n-j} |0\rangle^j |1\rangle^{n-j} \quad (2)$$

The first factor of $|1\rangle^j$ denotes one photon in each of the first j modes of register x , and so forth. As illustrated in Figure 1, this corresponds to a superposition of terms in which there are j photons in x and $n - j$ in y , for a total of n photons in the two registers. The function $f(j)$ was not included in the original KLM approach and can be taken to have a constant value of 1 in that case. If the total number of photons after the Fourier transform is found to be equal to 0 or $n + 1$, the value of q has been measured and the results of the operation must be rejected in the original KLM approach. Failures of that kind occur with probability $1/(n+1)$. Because they occur in a known way, these failures can be corrected using a simple 2-qubit code with a probability P_C , although arbitrary errors cannot be corrected by such a code [1].

As we showed in an earlier paper [2], an alternative approach is to always accept the output of the logic operation (no post-selection) and choose the coefficients $f(j)$ to maximize the fidelity of the output. In that case, the probability of a teleportation error is reduced to approximately $2/(n+1)^2$ in the limit of large n , which can be seen to be roughly the square of the failure rate in the original KLM approach. Unlike the failures in the KLM approach, there is no independent indication of the occurrence of such an

error, but they can be corrected using the 7-qubit Steane code [12], for example. The original KLM approach and our high-fidelity approach both have potential advantages and disadvantages, and the optimal method will probably depend on a number of factors, including the application and the range of values of n that can be generated. As an example, the high-fidelity approach allows the teleportation of a single-photon state with the smallest possible error for a given value of $n > 1$.

A controlled sign gate (a controlled Pauli operator \hat{Z}) can be implemented by teleporting two qubits q and q' using two sets of entangled ancilla registers, x, y, x' , and y' , as illustrated in Figures 1 and 3. The two qubits are teleported independently as described above, but the two sets of ancilla are now assumed to be in an entangled state of the form

$$|\psi_{AA'}\rangle = \sum_{j=0}^n f(j) |1\rangle^j |0\rangle^{n-j} |0\rangle^j |1\rangle^{n-j} \sum_{j'=0}^n (-1)^{jj'} f(j') |1\rangle^{j'} |0\rangle^{n-j'} |0\rangle^{j'} |1\rangle^{n-j'} \quad (3)$$

It can be seen that this is the tensor product of two ancilla states of the form given in Eq. (2), aside from the factor of $(-1)^{jj'}$ which entangles the two. The teleportation proceeds as before, with the two output qubits selected from the modes of registers y and y' as illustrated in the figure. An additional deterministic sign correction may be required based on the results of the measurements of the numbers of photons after the Fourier transforms. A controlled sign gate can be used to implement a controlled-NOT gate by inserting it into one arm of an interferometer. The two beam splitters in such an interferometer are each equivalent to a Hadamard transformation \hat{H} aside from single-qubit phase shifts.

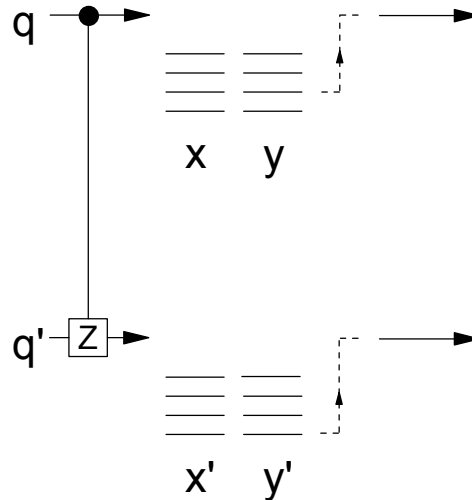


Figure 3. Implementation of a controlled sign gate (controlled \hat{Z}) by teleporting input qubits q and q' using entangled ancilla registers x, y, x' , and y' . Each of the output qubits is selected from registers y or y' based on the results of the measurements, as indicated by the dashed lines.

Up to this point, we have assumed that each of the logical qubits is represented by a single photon. But scalable quantum computing will require the ability to use encoded qubits combined with quantum error correction [12, 13, 14] and fault-tolerant logic operations [10, 15, 16]. Each logical qubit can be encoded into k physical qubits, each of which will be represented by a single photon in the case of linear optics quantum computing. Each of those qubits could be further encoded into k physical qubits, forming a concatenated code with l layers. For simplicity, we will only consider error-correcting codes for which the encoded controlled-NOT operation consists of applying a controlled-NOT to corresponding pairs of physical qubits at the lowest level of the code. It will also be assumed that the encoded forms of the Hadamard operator \hat{H} and Pauli operators \hat{X} and \hat{Z} consist of applying the corresponding single-qubit operators to each of the physical qubits. These properties are satisfied by the 7-qubit Steane code [12], for example.

Two somewhat different strategies can be used to implement fault-tolerant quantum computation using linear optics. We have suggested a “bottom-up” approach that is based on the fact that the theory of fault-tolerant error correction does not depend on the physical nature of the logic devices, provided that the necessary logic operations can all be done with an error probability P_E per operation that is below some threshold probability P_T [10, 15, 16]. For example, if $P_T \sim 10^{-4}$, then the threshold could be met using the high-fidelity approach and $n \sim 200$, which would give $P_E < P_T$ provided that the other sources of error in a single controlled-NOT operation are sufficiently small. In this approach, the controlled sign gate described above would be combined with Hadamards to implement the controlled-NOT operation between the physical qubits at the lowest level of the code. The optical components, ancilla, Fourier transform, and measurements can best be viewed as a compound “device”, in analogy with the physical devices used to implement a CNOT gate in other implementations, such as the Kane approach [17], for example.

Although this would appear to be a straightforward application of standard fault-tolerant computational techniques, it may be useful to describe this approach in a little more detail. A sufficient set of fault-tolerant operations consists of \hat{H} , the controlled-NOT, the phase gate \hat{S} , and the $\pi/8$ gate \hat{T} , where the latter two gates are defined as usual [10] by

$$\hat{S} = \begin{pmatrix} 1 & 0 \\ 0 & i \end{pmatrix} \quad \hat{T} = \begin{pmatrix} 1 & 0 \\ 0 & e^{i\pi/4} \end{pmatrix} \quad (4)$$

The encoded form of \hat{H} is straightforward to implement, since it can be applied bit-by-bit to the physical qubits, where it can be implemented using a beam splitter and phase shifters. The encoded form of \hat{S} is almost as simple to implement, since it consists of

applying $\hat{Z}\hat{S}$ to each of the physical qubits [10], while \hat{Z} and \hat{S} are both simple single-qubit operations on the physical qubits. The encoded form of the controlled-NOT can be implemented by applying two Hadamards and a controlled- \hat{Z} operation on each pair of physical qubits as described below. For unencoded qubits (single photons), \hat{T} is also a simple linear transformation that could be applied using a phase shifter, but its encoded form requires the use of an ancilla, a CNOT gate, and a measurement [10]. Thus the standard set of fault-tolerant gates can be implemented provided that we have an encoded form of the CNOT gate.

It follows from the properties of the encoded \hat{H} and CNOT that an encoded controlled- \hat{Z} operation can also be performed bit-by-bit on two encoded qubits as illustrated in Figure 4. A 2-qubit encoding is illustrated for simplicity, although the same procedure can be applied for arbitrary values of k . The controlled- \hat{Z} operation is applied consecutively to each pair of physical qubits at the lowest layer, although the figure only shows it being applied to one such pair. A separate set of entangled ancilla of the form shown in Eq. (3) is required to teleport each pair of physical qubits while applying the desired logical operation. It should be emphasized that the ancilla used in this process are not encoded, and the logical operation between each pair of physical qubits is exactly as described above. For reasons that should become apparent shortly, we will refer to unencoded ancilla of this kind that are used to perform two-qubit operations on the physical qubits via teleportation as “resource ancilla”.

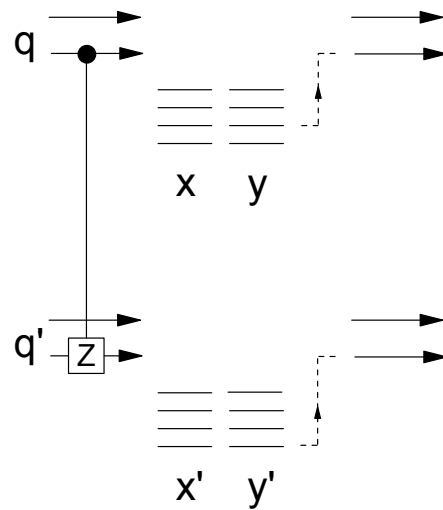


Figure 4. A controlled sign operation applied to two encoded qubits q and q' . The controlled- \hat{Z} operation is applied individually to each pair of physical qubits using the teleportation technique described above. A 2-qubit encoding is shown for simplicity, although the same procedure applies for larger values of k . In addition, the same procedure can be also be applied to the lowest layer of a concatenated encoding, while only a single layer of encoding is shown here.

Using the encoded form of the operators described above, fault-tolerant quantum computation can be performed using standard techniques [10, 15, 16] provided that the error in each of these operations is less than P_T . It should be emphasized once again that this approach makes use of logical qubits that are encoded while the resource ancilla are not encoded.

It would be desirable to be able to generalize linear optics quantum computing to allow the use of encoded ancilla for quantum logic operations, since that would make the ancilla relatively insensitive to decoherence during their generation, transportation, storage, and measurement. In order to understand the limitations in this process, it is instructive to consider the generalization of the high-fidelity approach to use encoded ancilla, as illustrated in Figure 5. Here each of the logical 0s and 1s in the ancilla are represented by a concatenated encoding of k physical qubits in l layers in exactly the same way as are the logical qubits. This is an example of a “top-down” approach to fault-tolerant computation, where we start with the original logic process, encode both the qubits and ancilla, and develop encoded versions of all of the required operations, including the Fourier transform.

To be more specific, the entangled ancilla states are now assumed to have the form

$$|\psi_{AA'}\rangle = \sum_{j=0}^n f(j) |1_L\rangle^j |0_L\rangle^{n-j} |0_L\rangle^j |1_L\rangle^{n-j} \sum_{j'=0}^n (-1)^{jj'} f(j') |1_L\rangle^{j'} |0_L\rangle^{n-j'} |0_L\rangle^{j'} |1_L\rangle^{n-j'} \quad (5)$$

where $|0_L\rangle$ and $|1_L\rangle$ represent the corresponding encoded form of the logical qubits. The teleportation is performed in such a way that an entire encoded block is selected based on \hat{F} and subsequent measurements to form the output, aside from the necessary phase corrections. As we will see in more detail in Section V, this approach is fault-tolerant but it is limited by the fact that the encoded form of the Fourier transform is no longer a simple linear transformation as it is for unencoded photonic qubits. In fact, the encoded form of \hat{F} requires the use of CNOT gates at the level of the physical qubits, which is analogous to the properties of the simple single-qubit operator \hat{T} . The required CNOT operations can be applied to the physical qubits using unencoded ancilla and teleportation as described above, which is why we previously referred to unencoded ancilla used in this way as resource ancilla.

It can be seen that this top-down approach leads to two types of ancilla, those used at the upper, logical level of the code and the resource ancilla used to perform two-qubit operations between the physical qubits at the lowest level of the code. If our goal is to implement a controlled- Z operation, then it would appear to be more efficient to implement it directly using unencoded qubits, as in Figure 4.

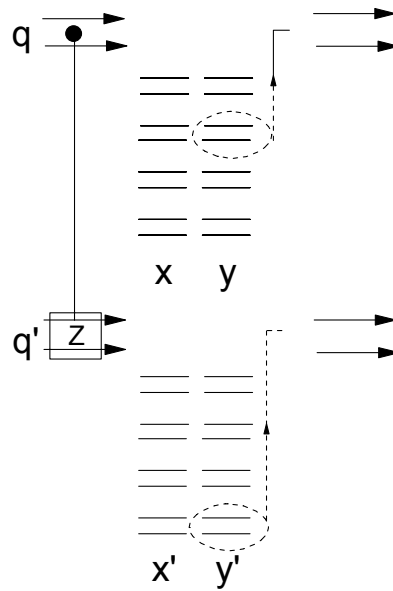


Figure 5. Schematic illustration of the generalization of the high-fidelity approach to use encoded ancilla states. Here an entire encoded block corresponding to one logical qubit of the ancilla is selected as the output of the device. This requires that the logical qubits and ancilla be encoded in the same way. It is shown in Section V that the transfer of an entire block to the output can be performed in a fault-tolerant way, but that the encoded form of the Fourier transform is no longer a simple linear transformation.

The above example suggests that it may not be possible to eliminate the use of unencoded ancilla in linear optics quantum computing. That conclusion is further illustrated by the top-down approach to fault-tolerant computation described by KLM [1, 18]. Their approach starts with the teleportation method of Gottesman and Chuang [6] using EPR pairs as the ancilla, which is equivalent in some sense to the case of $n=1$. The qubits and the EPR ancilla are assumed to be encoded in the same way using a 2-qubit concatenated code. In the set of fault-tolerant gates, the controlled-NOT is replaced with the operator $(ZZ)_{90}$, which is equivalent to a controlled- \hat{Z} gate aside from single-qubit rotations. After $(ZZ)_{90}$ has been pushed back through the teleportation and applied to the ancilla using post-selection, KLM concentrate on making the individual teleportations fault-tolerant. The teleportation of the physical qubits relies on the use of another two-qubit gate, $(ZY)_{90}$, that can also be related to a controlled- \hat{Z} and can be implemented by teleporting the physical qubits using unencoded ancilla and a Fourier transform as described above. The net result is that the teleportation of the encoded logical ancilla in the Gottesman-Chuang scheme requires the use of unencoded resource ancilla, just as in the earlier example of Figure 5. The difficulty in avoiding the use of unencoded ancilla is discussed in more detail in Section V.

One potential advantage of this approach is the fact that the intrinsic failure rate for teleportation is $1/(n+1)$ whereas it is $2/(n+1)$ for a CNOT; the lower error rate makes it easier to meet the threshold for fault-tolerant computation for small values of n . In addition, there is a straightforward way to correct the z-measurement failures in teleportation with a probability P_C , which allows the use of a 2-qubit code if the most

general sources of error can be neglected; a 2-qubit code can correct for several other sources of error as well but not for a bit-flip error, for example. As a result, KLM were able to obtain fault-tolerant computation for $n = 3$ in the ideal case of no arbitrary errors [1].

In order to include the effects of arbitrary errors in this kind of approach, one might envision a concatenation of several layers of a 7-qubit code, which is able to correct for arbitrary errors, with further layers of a 2-qubit code below that to reduce the effects of z-measurement failures. Let N_2 be the total number of operations required in the 2-qubit layers of the code in order to reduce the error rate due to z-measurement failures to less than P_T at the upper level of the 2-qubit code. Then the error rate per logic operation on the physical qubits due to the most general form of error would have to be less than P_T / N_2 for fault-tolerant computation, since those errors cannot be corrected by a 2-qubit code.

By way of comparison, fault-tolerant computation using the high-fidelity approach would require that the error probability in performing a single CNOT operation using n ancilla photons must be less than P_T . This would require $n \sim 200$ for a frequently-quoted estimate of P_T . The relative advantages and disadvantages of the two approaches depend to a large extent on the availability of ancilla states with specific values of n , which is the subject of the next three sections.

III. POST-SELECTION

As we saw in the previous section, either approach to linear optics quantum computing [1, 2] will require teleportation using ancilla photons in the unencoded state shown in Eq. (3). The most straightforward way to generate these states is to use elementary logic gates, such as a probabilistic controlled-NOT, combined with post-selection. The ancilla required for the elementary gates consist of either single photons or the two-photon Bell-state $|\Phi^+\rangle$. Assuming that these states are available [19, 20, 21] as a basic resource, then the entangled ancilla state of Eq. (3) can be generated using the techniques described in this section.

The elementary gates that have been proposed include a nonlinear sign gate [1], several forms of controlled-NOT gates [22, 23, 24, 25], parity checks [23], quantum encoders [23], and QND measurements [26]. We have experimentally demonstrated [27, 28] quantum parity checks, encoders, and controlled-NOT gates that succeed with probabilities ranging from $1/4$ to $1/2$. The existing experiments were performed in the coincidence basis, but that restriction can be removed once a reliable source of single-photons and $|\Phi^+\rangle$ states becomes available [21].

The generation of the entangled ancilla state can be performed in three steps: (a) Generation of a single photon in each mode of registers y and y' . (b) Conditional transfer of single photons from register y to x and from y' to x' . (c) Entanglement of the two sets

of registers by applying a phase shift of $(-1)^{j'}$. Each of these steps will now be described in more detail.

A. Generation of single photons in y and y'

The first step in the generation of the required ancilla state is to transfer a single photon into each mode of the y and y' registers, as illustrated in Fig. 6. (It is assumed that all of the registers were in the vacuum state initially.) A number of single-photon sources have been experimentally demonstrated [29, 30, 31, 32]. If each mode of the two registers consists of a single-mode optical fiber, then the photons can simply be routed from the single-photon sources into the appropriate fibers.

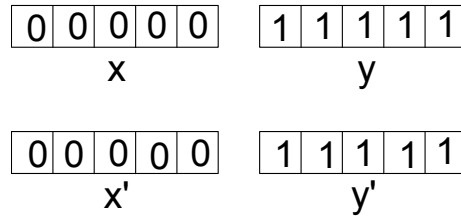


Figure 6. The first step in the generation of the entangled ancilla state is the transfer of a single photon into each mode of registers y and y' .

An error in the subsequent logic operations will occur if the single-photon source fails to generate a photon as expected. As a result, the efficiency of the single-photon source is an essential requirement for fault-tolerant quantum computing. An ideal way to achieve high efficiencies would be to generate a pair of photons directly in an optical fiber using down-conversion, which would avoid any coupling losses [33]. The detection of one member of the pair would then ensure that the other photon is present in the fiber with high probability.

B. Conditional transfer of photons

The next step in the generation of the entangled ancilla consists of conditional transfers of photons from register y to x and from register y' to x' in order to create two independent ancilla of the form shown in Eq. (2). For example, we first need to transfer the photon initially in the left-most mode of y into the left-most mode of x with the appropriate probability amplitude, as illustrated in Fig. 7. This process must create a coherent superposition of the two states, but it will be convenient to describe the process in terms of the probability P_1 that the photon would be found in x after the process has been completed. The required value of P_1 will be specified shortly.

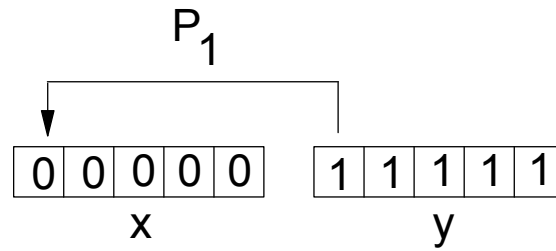


Figure 7. Coherent transfer of a single photon from register y to the appropriate mode of register x with probability P_1 .

Once the first photon has been transferred with probability P_1 , a second photon must be transferred with probability P_2 from the second mode from the left-hand-side of register y to the corresponding mode in register x, as illustrated in Figure 8. This process is conditional, however, in the sense that it is to be performed only if the first transfer was successful, i.e., only if the first mode of register x actually contains a photon. Once again, this process, if applied, produces a coherent superposition state, although it is convenient to describe it in terms of the corresponding probability P_2 that the second photon would be found in x.

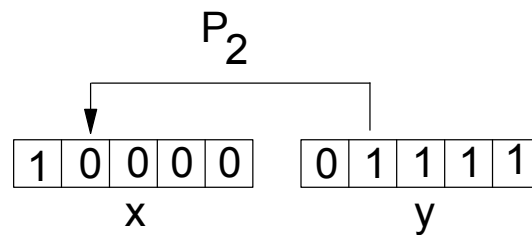


Figure 8. Conditional transfer of a photon from one mode of register y to the corresponding mode of register x. This process only takes place if the first mode in register x contains a photon, in which case it creates a superposition of states in which the second photon would be found in register x with probability P_2 .

Conditional photon transfers of this kind can be implemented using the interferometer shown in Figure 9. Here the solid lines represent mirrors, the dashed lines represent 50/50 beam splitters, the modes have been labeled a through f, and ϕ is a phase shift of either 0^0 or 180^0 . If a photon is initially present in path a, the initial state of the system is

$$|\psi\rangle = \hat{a}^\dagger |0\rangle \quad (6)$$

Here the operators \hat{a}^\dagger , \hat{b}^\dagger , etc., create a single photon in the corresponding mode, as usual. The first beam splitter applies the operator transformation

$$\begin{aligned}\hat{a}^\dagger &\rightarrow T\hat{d}^\dagger + iR\hat{c}^\dagger \\ \hat{b}^\dagger &\rightarrow T\hat{c}^\dagger + iR\hat{d}^\dagger\end{aligned}\quad (7)$$

where R and T are the reflection and transmission coefficients of the beam splitter (both real numbers). The phase shifter applies the transformation

$$\hat{d}^\dagger \rightarrow \exp[i\phi]\hat{d}^\dagger \quad (8)$$

after which the second beam splitter applies the transformation

$$\begin{aligned}c^\dagger &\rightarrow T\hat{f}^\dagger + iR\hat{e}^\dagger \\ \hat{d}^\dagger &\rightarrow T\hat{e}^\dagger + iR\hat{f}^\dagger\end{aligned}\quad (9)$$

After these transformations the output state reduces to

$$\begin{aligned}|\psi_{out}\rangle &= -\hat{e}^\dagger |0\rangle \quad \text{for } \phi = 180^\circ \\ |\psi_{out}\rangle &= [-(1-2T^2)\hat{e}^\dagger + 2iRT\hat{f}^\dagger] |0\rangle \quad \text{for } \phi = 0^\circ\end{aligned}\quad (10)$$

It can be seen that the incident photon always appears in the output mode e if $\phi = 180^\circ$, while it is transferred to mode f with probability $4R^2T^2 = 4(1-T^2)T^2$ if $\phi = 0^\circ$. By choosing the proper value of T, it is thus possible to transfer the photon with any desired probability P provided that $\phi = 0^\circ$.

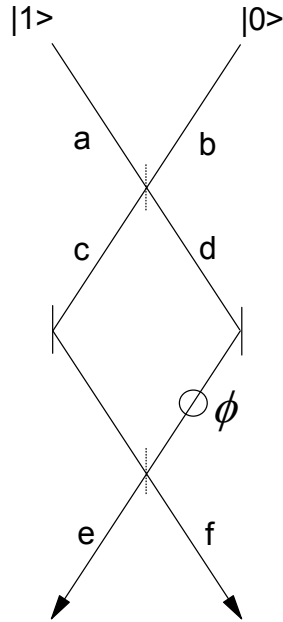


Figure 9. Interferometer arrangement used to implement the conditional photon transfer of Figure 8. A photon initially present in path a will be transferred to path f with probability amplitude $2iRT$ if $\phi = 0^\circ$, while it will exit with certainty in path e if $\phi = 180^\circ$.

The value of ϕ can be set to one of these two values using the controlled sign gate described above, where the control qubit is located in the y mode from the previous conditional transfer (or the x mode with a fixed 180° phase shift). The choice of the appropriate values of R and T will allow each of the successive transfers to occur with the desired probability amplitude, provided that the previous transfer occurred. The correct value of P_1 corresponds to the sum over all of the states with one photon in the first mode of x, regardless of the occupation of the other modes:

$$P_1 = \sum_{j=1}^n f^2(j) \quad (11)$$

Here $f(j)$, a real number, is either a constant in the original KLM approach [1] or chosen to maximize the fidelity as described in Ref. [2].

The required value of P_2 corresponds to the total probability of all states having a photon in mode 2 of x, given that mode 1 is occupied. The fact that mode 1 is assumed to be occupied requires the introduction of a normalized probability amplitude $f'(j)$ given by

$$f'(j) = \frac{f(j)}{\left(\sum_{j'=1}^n f(j')^2\right)^{1/2}} \quad (12)$$

The necessary value of P_2 is then given by

$$P_2 = \sum_{j=2}^n f'(j)^2 \quad (13)$$

This process is then repeated for the remaining modes of x , which populates each term in the superposition with the correct probability amplitude and leaves the system in the entangled state of Eq. (2), as desired. An identical procedure is also applied to registers x' and y' to prepare them in the same entangled state.

The generation of two sets of entangled states of this kind requires a total of $2(n-1)$ controlled sign gates, since the first transfer in each register is not conditional.

C. Entanglement of the two sets of registers

The final step in the creation of the entangled ancilla is the application of a factor of $(-1)^{jj'}$, which entangles the two sets of registers as required in Eq. (3). Two different procedures can be used, depending on the magnitude of n .

If n is relatively small, the most efficient way to apply this phase shift is to perform n^2 controlled sign gates between each pair of qubits in x and x' , with the x qubit the control and the x' qubit the target [1]. If we look at any given term in Eq. (3) with specific values of j and j' , it can be seen that a minus sign will be applied a total of jj' times, as required.

For large values of n , it is more efficient to avoid the quadratic dependence on n by measuring the parities of registers x and x' . This is based on the observation that jj' will be even if either j or j' is even, whereas it will be odd only if both j and j' are odd. The parity of register x can be obtained by introducing an additional ancilla qubit q_a that is initially in the state 0, and then successively applying a CNOT gate between q_a and every qubit in x , with the x qubits the control and q_a the target. The ancilla will then have the value 0 if x has even parity and 1 if x has odd parity. The parity of x' can be determined in the same way using a second ancilla q_b .

Having determined the parities of x and x' , we introduce a third ancilla q_c initially in the state 0 and apply a controlled-controlled-NOT gate (Toffoli gate) to q_c with q_a and q_b as the controls. (This operation can be performed using CNOTs and single-qubit operations.) Ancilla q_c will now have the value 1 if and only if both j and j' are odd, so that the factor of $(-1)^{jj'}$ can now be applied by using a controlled sign gate applied to qubit 1 of registers x and y with q_c as the control.

In order to avoid any entanglement between the terms in Eq. (3) and the states of the ancilla q_a , q_b , and q_c , it is also necessary to return all of these ancilla to the state $|0\rangle$. This can be done by repeating the controlled-controlled-NOT a second time, applying n CNOTs between q_a and the qubits of x , and applying n CNOTs between q_b and the qubits of x' . Including these operations, a total of $4n$ CNOT operations are required to apply the factor of $(-1)^j$ in the limit of large n .

D. Overall efficiency

Using $|\Phi^+\rangle$ states as a resource [21], controlled-NOT gates can be implemented using polarization techniques [23] with a probability of success of $1/4$. Controlled phase gates can be implemented directly using an interferometric approach [1, 25] with a probability of success of $1/16$. It is more efficient, however, to implement the controlled phase gates using two Hadamards and a polarization-based CNOT, which allows the controlled sign gates to be implemented with a probability of success of $1/4$ as well.

For the case of $n=3$, $2(n-1)=4$ conditional transfers using a controlled sign gate are required to create the independent ancilla of Eq. (2). An additional $n^2=9$ controlled sign gates are required to apply the factor of $(-1)^j$. Thus the probability $P_s(3)$ of successfully generating an $n=3$ set of entangled ancilla is given by

$$P_s(3) = \left(\frac{1}{4}\right)^{13}. \quad (14)$$

In the limit of large n , $2(n-1)$ controlled sign gates are again required to create the independent ancilla, followed by $4n$ controlled-NOTs to apply the factor of $(-1)^j$. The corresponding probability of success is given by

$$P_s(n) = \left(\frac{1}{4}\right)^{6n-2} \quad (n \gg 1) \quad (15)$$

The fixed number of operations required for the controlled-controlled-NOT gates are insignificant in the limit of large n and have not been included in Eq. (15).

It can be seen that the number of attempts required to successfully generate the required ancilla state using post-selection increases exponentially with the value of n and is relatively large even for the case of $n=3$. It may be possible to improve on this result considerably by generating the ancilla in an encoded basis and then decoding them for subsequent use, as is discussed in Section V. It should also be noted that we have not proven that this method is optimal, and the possibility remains that there may be more efficient methods, especially for small values of n .

IV. SOLID-STATE TECHNIQUES

In this section, we consider the possibility of generating the required ancilla states using solid-state techniques. One possible approach based on the use of quantum dots [34, 35] and the Coulomb blockade effect [3, 4] is suggested. A detailed analysis of practical issues, such as decoherence and the necessary micro-fabrication techniques, is beyond the intended scope of this paper.

The basic structure of interest is shown in Figure 10 for the case of $n=3$, although the method is easily generalized to larger values of n . Each qubit in registers x and y are represented by a quantum dot labeled D_1 through D_6 in the figure. A thermal reservoir containing a large number of electrons is located on the right-hand-side of the array of quantum dots. The reservoir and each of the dots are separated by a tunnel barrier whose height can be controlled by applying an electrostatic potential to a series of gates labeled B in the figure. The quantized energy levels in each of the dots can be controlled using another set of gates labeled U , which would be placed above or below the dots to produce a uniform electrostatic potential.

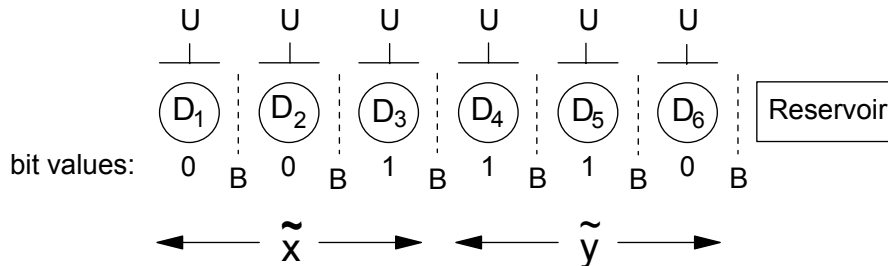


Figure 10. Generation of a photonic ancilla state by first generating the corresponding entangled state of n electrons in a series of quantum dots labeled D_1 through D_6 . The B gates are used to control the height of a tunneling barrier between the quantum dots, while the U gates are used to control the energies of the quantized states within each dot. A typical set of bit values is also shown below each quantum dot.

The goal is to first create an entangled state of n electrons as given in Eq. (3), where the presence of an excited electron will represent a logical value of 1 while the absence of an electron will represent the logical value 0. The electrons will be assumed to be in an excited state that allows the emission of a single photon into a single-mode optical fiber, so that the entangled state can be transferred to a photonic state if the coupling is sufficiently efficient [5]. In order to avoid the emission of photons during the time that the electronic state is being prepared, it may be necessary to first set up the electronic state in a set of quantum dots that are not coupled to the fibers and then simultaneously transfer all of the electrons to another set of quantum dots (not shown in the figure) that are coupled to the fiber modes.

The registers x and y have been rotated through an angle of 180° compared to Figure 1, so that all of the 1s in the x register are now on its right-hand-side, while all of the 1s in the y register are now on its left-hand-side; the rotated registers have been denoted by \tilde{x} and \tilde{y} . As a result of this rotation, all of the 1s are in adjacent locations and will form a contiguous block of n excited electrons after the electronic state has been prepared, as illustrated by the bit values shown in Fig. 10.

The first step is to put all of the quantum dots into the logical state 0, which can be accomplished by raising their electrostatic potential and putting them into thermal equilibrium with the reservoir. A single excited electron can then be transferred from the reservoir to quantum dot D_6 using standard techniques in which the height of the tunnel barrier is reduced and the two regions are coupled for a time interval Δt chosen to produce a complete Rabi oscillation. The transfer of two electrons in this process is prohibited by energy conservation, as has been demonstrated experimentally [3, 4]. Similar Rabi oscillations can then be used to transfer a single electron into registers D_4 and D_5 . At this point, all of the qubits in register \tilde{y} have the value 1, in analogy with Fig. 6.

Once the \tilde{y} register has been filled with single electrons, the next step in the process is to adjust the height of the tunnel barrier between quantum dots D_3 and D_4 to perform a partial Rabi oscillation. This interaction is applied for a time interval $\Delta t'$ chosen in such a way that an electron will be transferred between the two quantum dots with a probability P_1 as specified in Eq. (11). If the transfer occurred, we need to perform a sequence of complete Rabi oscillations between successive quantum dots in register \tilde{y} in order to move the missing electron (logical 0) all the way to the right, as illustrated in Figure 10. Since the first transfer may or may not have occurred, this process must be applied in any event and may therefore involve Rabi oscillations between two quantum dots that both contain an electron. In that case, the system is never left with two electrons in one of the dots and zero in the other because that is prohibited by the Coulomb blockade effect (energy conservation). The entire process is then repeated with probability P_2 and so forth until all of the terms in the superposition state of Eq. (2) have been generated with the appropriate probability amplitudes.

Similar techniques are also used to generate the same entangled state in a second set of rotated registers \tilde{x}' and \tilde{y}' (not shown). The factor of $(-1)^{j'}$ can then be applied using the Coulomb interaction between the electrons in register \tilde{x} and those in register \tilde{x}' . We assume that the electrons in registers \tilde{y} and \tilde{y}' are shielded with grounded conductors so that there is no interaction between their two sets of charges. We also note that the Coulomb interaction between the electrons within register \tilde{x} itself will produce an undesired phase shift, but that depends only on the value of j and can therefore be cancelled out by applying an appropriate set of potentials to the U gates; the same can be done for register \tilde{x}' . With these precautions, the net electrostatic interaction is proportional to the product of the sum of the charges on \tilde{x} and \tilde{x}' , which is proportional

to jj' . (This assumes that the distance between the two registers is much larger than the separation of quantum dots within a register.) Under these conditions, the factor of $(-1)^{jj'}$ can thus be applied by simply waiting for an appropriate time interval.

Aside from practical issues such as decoherence, the above discussion shows that solid-state systems of this kind can be used in an efficient way to generate the entangled states that are required for linear optics quantum computing. Quantum-dot techniques have also been proposed as a scalable approach to quantum computing [34, 35, 36]. Our results suggest the possibility of a hybrid approach that may be able to combine the potential advantages of both solid-state and linear-optics techniques. This is especially true of intermediate-range applications in quantum communications that may be much less demanding than the construction of a full-scale quantum computer. For example, a quantum repeater or relay system with an error of a few percent could be constructed using high-fidelity [2] quantum logic gates operating with ancilla from a quantum dot array with $n \sim 10$.

V. ENCODED ANCILLA

It would obviously be desirable to be able to use encoded ancilla in linear optics quantum computing applications in order to reduce the effects of decoherence and other error sources in the generation, transportation, storage, and measurement of the ancilla. As we briefly mentioned in Section II, it does not appear to be possible to avoid the use of unencoded ancilla in the teleportation of the physical qubits. In this section, we consider this issue in a little more detail and also investigate the possible advantages of generating the ancilla in an encoded basis and then decoding them for use in the logic gates.

One potential way to generalize linear optics quantum computing to allow the use of encoded ancilla would be to take the entire teleportation algorithm of Fig. 3 and replace all of the original qubits with encoded qubits, as illustrated in Fig. 5. This requires that all of the necessary operations, including the Fourier transform and the phase corrections, be replaced with their encoded forms [10], as was discussed briefly in Section II.

The first difficulty that arises in such an approach is the fact that the Fourier transform defined in Eq. (1) can produce two or more photons in a single mode of registers q and x . This takes the system out of the vector space spanned by the qubits, which correspond to either 0 or 1 photons in each mode. One solution to this problem is to introduce a second register z containing m modes, where m is a multiple of $n+1$, the number of modes in q and x . (A more efficient method exists but will not be discussed here.) Once again, register z can be viewed as a bundle of m single-mode optical fibers. If we write $m = L(n+1)$, where L is a large integer, then we can consider a generalized Fourier transform \hat{G} defined in analogy with Eq. (1) by

$$\hat{a}_j^\dagger = \frac{1}{\sqrt{m}} \sum_{k=1}^m e^{2\pi ijk/(n+1)} a_k^\dagger \quad (16)$$

This is a linear transformation that can also be implemented using a series of beam splitters or optical fiber couplers. It can be shown that \hat{G} satisfies the usual properties of discrete Fourier transforms, namely that

$$\frac{1}{m} \sum_{k=1}^m e^{2\pi i k(j-j')/(n+1)} = \delta_{jj'} \quad (17)$$

It follows from this that \hat{G} has the same cyclic property [1] regarding a shift of the input qubits as does \hat{F} , so that teleportation can be performed in the same way as before by measuring the number of photons in each mode of z and selecting the output of the teleportation from the appropriate encoded qubit in ancilla y . In the limit of large L , the probability of finding two or more photons in a single mode of z goes to zero, so that the transformation leaves the system in the vector space spanned by the qubits.

Any unitary transformation such as \hat{G} can be implemented in a fault-tolerant manner [10], which means that the appropriate encoded form of \hat{G} can be determined and implemented on the encoded qubits. Unfortunately, the encoded form of an operator will in general involve a number of controlled-NOT operations, and this can be shown to be the case for \hat{G} . Thus we must be able to implement controlled-NOT operations on corresponding pairs of the physical qubits that comprise the ancilla, which in turn requires that we perform quantum teleportation as usual using a set of n' unencoded ancilla, or resource ancilla. The values of n and n' do not need to be related in any way, except that we must be able to meet the threshold P_T for fault-tolerant computation. A similar situation exists for the phase corrections that may be required depending on the results of the measurements, and they can be shown to require the use of controlled-NOT gates in their encoded form as well.

It should be noted that the measurement of the number of photons in each mode of z as well as the selection of the output qubit from one of the qubits in y is a fault-tolerant process. In analogy with the fault-tolerant measurements required for the standard implementation [10] of a $\pi/8$ gate, for example, the result of each measurement is a classical number whose error probability decreases exponentially with the number of layers of concatenation, while the transfer of the appropriate ancilla to the output can be performed bit-by-bit using the physical qubits. As a result, a single error will produce at most one error in any block of data, as required for fault-tolerant computation.

In this example, we introduced encoded ancilla qubits in an attempt to perform a controlled- \hat{Z} or controlled-NOT operation with reduced sensitivity to errors in the ancilla, but we found that we still needed to perform controlled-NOT operations on the physical qubits using unencoded resource ancilla. The latter will introduce their own errors, and there is no apparent advantage in such an approach, with the possible exception of certain communications protocols where the entangled ancilla must be distributed over large distances.

As we noted in Section II, a similar situation occurs in the 2-qubit encoding suggested by KLM [1], where logical EPR-state ancilla are used in the upper level of the code but the actual teleportation of the physical qubits must once again be done using unencoded resource ancilla. This appears to be a general limitation of linear optics quantum computing. Rather than attempt a proof, it may be more instructive to consider what would be required in order to perform an encoded form of \hat{F} or \hat{G} using a series of beam splitters. If single (unencoded) photons were passed through such a series of beam splitters, there would be some set of probability amplitudes to find the photons in each of the output modes. If the single photons were replaced with a logical qubit consisting of a block of single photons, then the corresponding logical output would consist of having the same set of probability amplitudes for the blocks of photons. This would require that they propagate through the beam splitters as if they were a bound system, such as a molecule. Although the diffraction of surprisingly large molecules by gratings has been experimentally demonstrated [37], for example, there is nothing to hold a block of photons together as a group, and a simple linear transformation no longer gives the desired result for encoded qubits.

The use of encoded ancilla may still be of some benefit in generating unencoded ancilla with large values of n . For example, suppose that a 2-qubit encoding can be used to implement fault-tolerant logic gates with $n'=3$, provided that the most general form of errors can be neglected up to a point. The generation of a set of encoded ancilla with a much larger value of n can be viewed as a unitary transformation, and it follows from the theory of fault-tolerant computation that this could be done with a negligible failure rate due to z-measurements. In other words, the failure rate of $(1/4)^{6n-2}$ can be avoided in such an approach but only because the ancilla are now in encoded form. These ancilla could then be decoded and used as a resource for other logic gates, such as the high-fidelity gates.

Errors in the decoding process can occur near the upper level of the code, where the encoding no longer protects the values of the qubits. In the limit of a small error probability P_D in decoding each bit, the total error probability P_A in a decoded ancilla would be $P_A = nP_D$. The simplest method of decoding would be to use the so-called destructive CNOT gate that we have experimentally demonstrated [27], which essentially erases any information regarding the control qubit in a coherent manner. This gate succeeds with a probability of $1/2$, so that the failure rate in decoding an encoded ancilla would be roughly given by

$$P_A \sim \left(\frac{1}{2}\right)^n \quad (18)$$

This estimate ignores failures in all but the highest level. A more detailed analysis would have to include failures in the lower levels in addition to the fact that they can be corrected with some probability as in the KLM gates, which would reduce the factor of $1/2$ somewhat. But even using a simple decoding of this kind, it is apparent that the success rate of Eq. (18) would be a considerable improvement over that of Eq. (15).

Finally, we note once again that fault-tolerant computation can be performed using encoded qubits and unencoded resource ancilla for both the KLM approach [1] and the high-fidelity approach [2], as discussed in section II.

VI. SUMMARY

In this paper, we have discussed several different methods for the generation of the entangled ancilla photon states required for linear optics quantum computing. Ancilla states with n photons can be generated in a straightforward way using elementary linear optics gates and post-selection. Given elementary CNOT gates that succeed with a probability of $1/4$ [23, 27, 28], this approach generates the correct ancilla state with a probability of $(1/4)^{6n-2}$ in the limit of large n . We have not shown that this method is optimal, however, and more efficient post-selection methods may eventually be found, especially for small values of n .

The possibility of using encoded ancilla states was investigated as a way to reduce their sensitivity to decoherence and to improve the efficiency with which they can be generated. It was found that the use of unencoded ancilla cannot be avoided because simple linear transformations, such as a phase shift or a Fourier transform, become nonlinear when applied to encoded qubits. The use of encoded ancilla may still be useful as an efficient method for generating ancilla with large values of n provided that they can be decoded for use in the actual logic gates.

We also suggested a possible solid-state approach for generating the entangled ancilla photon states. The corresponding entangled state of n electrons would first be generated using a series of quantum dots and tunnel barriers. The nonlinearity required for this process comes from the Coulomb blockade effect, which prevents more than one electron from being transferred to a single quantum dot. After the entangled state of the electrons has been generated, it would be transferred to n single-mode optical fibers using a set of efficient optical couplers [5].

The use of solid-state devices to generate the entangled ancilla photons suggests the possibility of a hybrid system that may combine the best features of both solid-state and linear optics devices. Hybrid systems of this kind may be a convenient way of initially implementing quantum communications systems whose requirements are more modest than that of a full-scale quantum computer. For example, a solid-state device capable of generating $n=10$ ancilla states combined with the high-fidelity approach [2] to quantum logic gates would allow the development of a quantum repeater [38] or relay [39] system based on teleportation with an error rate of a few percent.

We would like to acknowledge valuable discussions with Jonathan Dowling, Michael Fitch and Todd Pittman. This work was supported in part by funding from ARO, ARDA, ONR, NSA, and IR&D.

REFERENCES

-
- ¹ E. Knill, R. Laflamme, and G. J. Milburn, *Nature* **409**, 46 (2001).
- ² J. D. Franson, M. M. Donegan, M. J. Fitch, B. C. Jacobs, and T. B. Pittman, *Phys. Rev. Lett.* **89**, 137901 (2002).
- ³ A. Imamoglu and Y. Yamamoto, *Phys. Rev. Lett.* **72**, 210 (1994).
- ⁴ J. Kim, H. Kan, and Y. Yamamoto, *Phys. Rev. B* **52**, 2008 (1995).
- ⁵ It should be possible to achieve high coupling efficiency using a hemispherical micro-cavity and suitable dielectric coatings (M.G. Raymer, private communication).
- ⁶ D. Gottesman and I. Chuang, *Nature (London)* **402**, 390 (1999). See also M. A. Nielsen and I. L. Chuang, *Phys. Rev. Lett.* **79**, 321 (1997).
- ⁷ C. H. Bennett, G. Brassard, C. Crepeau, R. Jozsa, A. Peres, and W. K. Wootters, *Phys. Rev. Lett.* **70**, 1895 (1993).
- ⁸ L. Vaidman and N. Yoran, *Phys. Rev. A* **59**, 116 (1999).
- ⁹ N. Lutkenhaus, J. Calsamiglia, and K.A. Suominen, *Phys. Rev. A* **59**, 3295 (1999).
- ¹⁰ M. A. Nielsen and I. L. Chuang, *Quantum Computation and Quantum Information* (Cambridge U. Press, Cambridge, 2000).
- ¹¹ T. B. Pittman, B. C. Jacobs, and J. D. Franson, *Phys. Rev. A* **66**, 052305 (2002).
- ¹² A. M. Steane, *Phys. Rev. Lett.* **77**, 793 (1996).
- ¹³ P. W. Shor, *Phys. Rev. A* **52**, R2493 (1995); Proceedings of the 37th Annual Symposium on Fundamentals of Computer Science, pp 56-65 (IEEE Press, Los Alamitos, CA) 1996.
- ¹⁴ A.R. Calderbank and P.W. Shor, *Phys. Rev. A* **54**, 1098 (1996).
- ¹⁵ D. Gottesman, *Phys. Rev. A* **57**, 127 (1998).
- ¹⁶ J. Preskill, in *Quantum Information and Computation*, H.-K. Lo, T. Spiller, and S. Popescu, eds. (World Scientific, Singapore, 1998).
- ¹⁷ B.E. Kane, *Nature* **393**, 133 (1998).
- ¹⁸ E. Knill, R. Laflamme, and G. Milburn, *quant-ph/0006120* (2000).
- ¹⁹ P. Kok and S.L. Braunstein, *Phys. Rev. A* **62**, 064301 (2002).
- ²⁰ C. Sliwa and K. Banaszek, *quant-ph/0207117*.
- ²¹ T.B. Pittman, M.M. Donegan, M.J. Fitch, B.C. Jacobs, J.D. Franson, P. Kok, H. Lee, and J.P. Dowling, submitted to the IEEE Journal of Selected Topics in Quantum Electronics (JSTQE) issue on Quantum Internet Technologies, D. Jackson, J. Franson, G. Milburn, and G. Gilbert, Eds. (*quant-ph/0303113*).
- ²² M. Koashi, T. Yamamoto, and N. Imoto, *Phys. Rev. A* **63**, 030301 (2001).
- ²³ T. B. Pittman, B. C. Jacobs, and J. D. Franson, *Phys. Rev. A* **64**, 062311 (2001).
- ²⁴ K. Sanaka, K. Kawahara, and T. Kuga, *Phys. Rev. A* **66**, 040301 (2002).
- ²⁵ T.C. Ralph, A.G. White, W.J. Munro, and G.J. Milburn, *Phys. Rev. A* **65**, 012314 (2001).
- ²⁶ P. Kok, H. Lee, and J.P. Dowling, *Phys. Rev. A* **66**, 063814 (2002).
- ²⁷ T. B. Pittman, B. C. Jacobs, and J. D. Franson, *Phys. Rev. Lett.* **88**, 257902 (2002).
- ²⁸ T.B. Pittman, M.J. Fitch, B.C. Jacobs, and J. D. Franson, submitted to *Nature* (*quant-ph/0303095*).
- ²⁹ J. Kim, O. Benson, H. Kan, and Y. Yamamoto, *Nature* **397**, 500 (1999).
- ³⁰ C. Kurtsiefer, S. Mayer, P. Zarda, and H. Weinfurter, *Phys. Rev. Lett.* **85**, 290 (2000).
- ³¹ A. Beveratos, R. Brouri, T. Gacoin, J.-P. Poizat, and P. Grangier, *Phys. Rev. A* **64**, 061802 (2000).
- ³² T. B. Pittman, B. C. Jacobs, and J. D. Franson, *Phys. Rev. A* **66**, 042303 (2002).
- ³³ M. Fiorentino, P.L. Voss, J.E. Sharping, and P. Kumar, *IEEE Photonics Technology Letters* **14**, 983 (2002).
- ³⁴ G. Chen, T.H. Stievater, E.T. Batteh, L. Xiaoqin, D.G. Steele, D. Gammon, D.S. Katzer, D. Park, and L.J. Sham, *Phys. Rev. Lett.* **88**, 117901 (2002).
- ³⁵ H.-A. Engel, P. Recher, and D. Loss, *Solid State Communications* **119**, 229 (2001).
- ³⁶ N.E. Bonesteel, D. Stepanenko, and D.P. Divincenzo, *Phys. Rev. Lett.* **87**, 207901 (2001).
- ³⁷ B. Brezger, L. Hackermuller, S. Uttenthaler, J. Petschinka, M. Arndt, and A. Zeilinger, *Phys. Rev. Lett.* **88**, 100404 (2002).
- ³⁸ P. Kok, C.P. Williams, and J.P. Dowling, *quant-ph/0203134*.
- ³⁹ B.C. Jacobs, T.B. Pittman, and J.D. Franson, *Phys. Rev. A* **66**, 052307 (2002).